

dinitrophenol (DNP) was added during phase 1, 2, or 3. Oxygen uptake in each phase was stimulated by DNP. Maximal stimulation was obtained with $10\mu\text{M}$ DNP during phases 1 and 2, while $5\mu\text{M}$ DNP gave maximal stimulation during phase 3. The rate of respiration was approximately the same in all phases after the addition of DNP. In a typical experiment the rates of O_2 uptake were 1.5, 0.9, and $1.7\mu\text{l}/\text{min}$ in phases 1, 2, and 3, respectively. The DNP-stimulated rates for the three phases were between 2.6 and $2.7\mu\text{l}/\text{min}$. Thus, respiration during germination was probably limited by availability of adenosine diphosphate or endogenous inorganic phosphate, and the observed shifts in respiration may have resulted from altered concentrations of these compounds within the cells.

The higher respiration rates during phases 1 and 3 may be caused by increased utilization of adenosine triphosphate (ATP) in synthetic reactions. RNA (5), protein (6), and membranes (4, 7, 8) are formed in germinating pollen. Respiration during phase 1 may be activated by rapid synthesis of these materials in preparation for tube growth. Endogenous sucrose is hydrolyzed early in germination of lily pollen (9) so rapid phosphorylation of hexoses may stimulate respiration in phase 1. Adding glucose to ascites tumor cells stimulates respiration briefly because the glucose is rapidly phosphorylated (10).

Turnover of ATP may decrease before tube initiation, causing the low respiration of phase 2. Decreased ATP turnover could result from lowered rates of protein or membrane synthesis. Alternatively, sugar phosphates may accumulate during phase 1, depleting endogenous supplies of inorganic phosphate or free hexoses, which become limiting during phase 2.

Phosphorylations associated with growth of pollen tubes may stimulate respiration during phase 3. Cellulose, callose, and pectin are synthesized during tube growth (7, 11). Isolated plant enzymes form cellulose and callose from phosphorylated precursors (12), and the existence of phosphorylated intermediates in pectin synthesis has been postulated (13).

Germinating seeds and spores also undergo a transition from low to high rates of respiration, and the increased respiration is associated with the onset

of various metabolic activities. However, the respiratory pattern of germinating pollen is different from the patterns exhibited by seeds or spores. For example, germinating pea and bean seeds exhibit initial increases in respiration which occur as the seeds absorb water (14). Thereafter, respiration remains constant or decreases slightly until the radicle emerges, when further increases in respiration occur. Respiration of pea seeds seems to be limited by availability of oxygen before the radicle splits the seedcoat. Respiration of germinating pollen does not seem to have this limitation since DNP stimulates respiration. Spores from some fungi, including *Neurospora*, *Puccinia*, and *Ustilago*, absorb oxygen at increasing rates during germination (15). In contrast, the respiration of rapidly elongating pollen tubes is only slightly greater than the respiration of pollen during phase 1 before tubes have appeared.

DAVID B. DICKINSON

Department of Horticulture,
University of Illinois, Urbana 61803

References and Notes

1. J. Tupy, *Biol. Plant. Acad. Sci. Bohemoslov.* **2**, 169 (1960); E. Hrabetova and J. Tupy, *ibid.* **3**, 270 (1961); J. Tupy, *ibid.* **5**, 216 (1963).
2. J. L. Brewbaker and B. H. Kwack, in *Pollen Physiology and Fertilization*, H. F. Linskens, Ed. (North-Holland, Amsterdam, 1963), p. 143.
3. J. A. Goss, *Trans. Kansas Acad. Sci.* **65**, 310 (1962); R. G. Stanley and E. A. Lichtenberg, *Physiol. Plantarum* **16**, 337 (1963); J. L. Brewbaker and B. H. Kwack, *Amer. J. Botany* **50**, 859 (1963).
4. W. G. Rosen, S. R. Gawlick, W. V. Dashek, K. A. Siegesmund, *ibid.* **51**, 61 (1964).
5. S. Tano and H. Takahashi, *J. Biochem.* **56**, 578 (1964); J. P. Mascarenhas, *Amer. J. Botany* **6**, 617 (1965).
6. J. Tupy, in *Pollen Physiology and Fertilization*, H. F. Linskens, Ed. (North-Holland, Amsterdam, 1963), p. 86.
7. M. M. A. Sassen, *Acta Botan. Neerl.* **13**, 175 (1964).
8. D. A. Larson, *Amer. J. Botany* **52**, 139 (1965).
9. Y. Iwanami, *J. Yokohama Municipal Univ., Ser. C* **116** (Biol. 13), 1 (1959).
10. B. Chance and B. Hess, *J. Biol. Chem.* **234**, 2416 (1959); B. Chance and B. Hess, *ibid.* **234**, 2421 (1959).
11. G. Kessler, D. S. Feingold, W. Z. Hassid, *Plant Physiol.* **34**, 505 (1960); R. G. Stanley and F. A. Loewus, in *Pollen Physiology and Fertilization*, H. F. Linskens, Ed. (North-Holland, Amsterdam, 1963), p. 128.
12. D. O. Brummond and A. P. Gibbons, *Biochem. Biophys. Res. Commun.* **17**, 156 (1964); G. A. Barber, A. D. Elbein, W. Z. Hassid, *J. Biol. Chem.* **239**, 4056 (1964); D. S. Feingold, E. F. Neufeld, W. Z. Hassid, *J. Biol. Chem.* **233**, 783 (1958).
13. F. A. Loewus, *Nature* **203**, 1175 (1964).
14. S. P. Spragg and E. W. Yemm, *J. Exp. Botany* **10**, 409 (1959); H. Opik and E. W. Simon, *ibid.* **14**, 299 (1963).
15. A. S. Sussman, J. R. Distler, J. S. Krakow, *Plant Physiol.* **31**, 126 (1956); P. G. Caltrider and D. Gottlieb, *Phytopathology* **53**, 1021 (1963).
16. Supported in part by NSF grant GB 4239. The technical assistance of Bette Busch is gratefully acknowledged.

24 September 1965

"Negative" Crystals in Ice:

A Method for Growth

Abstract. *Holes bounded by crystallographic faces, or "negative" crystals, may be made in ice by inserting a hypodermic needle and connecting it to a vacuum. The evaporation habit changes as a function of temperature and growth rate. This procedure is a simple way of producing mirror-smooth, uncontaminated, crystallographic surfaces in compounds which have high vapor pressure.*

Negative crystals occur naturally and can be produced in several ways, but there has been no method of growing them.

Evaporation of ice crystals has received little study, with the exception of two short reports (1), several papers on thermal etching, and others on the condensation coefficient of ice at about -50°C (2). The standard etching technique for ice (3), however, is little more than a method of growing negative crystals at ice surfaces (4). Nakaya (5) has studied extensively the migration of naturally occurring negative crystals in ice in temperature gradients, but the migration is caused by both evaporation and condensation and is therefore difficult to interpret in terms of different crystal faces. The purpose of growing negative crystals was to determine relative evaporation rates on ice-crystal faces, but the ultimate achievement of this aim is doubtful. The method may, however, be useful as a simple way to produce large, pure, rather perfect faces on crystals which have high vapor pressure.

The only major equipment needed for growing negative crystals in ice is a walk-in cold room, a vacuum pump, and a supply of single crystals of ice. Large, exceptionally perfect (dislocation density 10^3 to 10^4 cm^{-2}) ice crystals from the Mendenhall Glacier in Alaska were used (6). A hole about 1 cm long, with a diameter slightly smaller than the outside diameter of the needle to be used, is drilled into a small block cut from a crystal by twirling the drill bit between a bare thumb and forefinger. (If a mechanical drill is used, it is difficult to avoid cracking the block.) The small end of a hypodermic needle that has been ground square and deburred is rested against the opening of the hole and

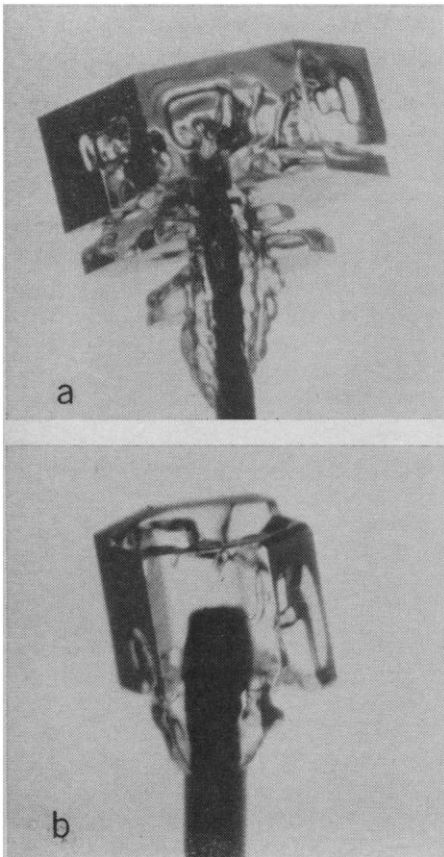


Fig. 1. Negative crystals in ice: holes evaporated from the ends of hypodermic needles embedded in solid ice. Outside diameter of needle in both is 0.4 mm. Control (not interface) temperature for *a*, -1.5°C ; for *b*, -4.6°C . Note the difference in evaporation habit. In both cases the *c*-axis is approximately parallel to the needle.

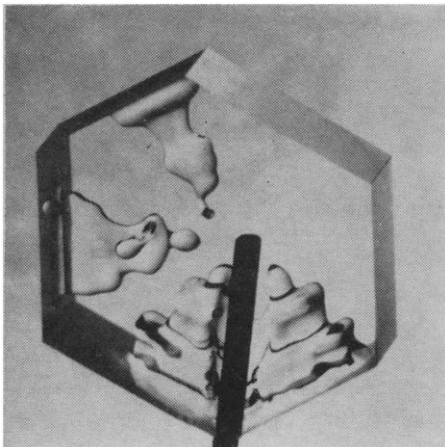


Fig. 2. Negative crystal growing at -14°C . The projections are rounded, the exterior portions angular. Note the asymmetry due to imperfect temperature control and the fact that the skeletal structure appears on the fastest-growing faces. The projections maintain themselves because of poor heat conduction to them, but eventually they are severed, and the pieces of ice fall to the bottom of the negative crystal. Needle diameter, 0.45 mm.

held in place by one finger on the connector end. The middle of the needle is gently heated with a small soldering iron, and a slight pressure gradually forces the needle into the hole. Glass windows are frozen on the specimen.

The specimen is enclosed in a constant-temperature chamber with windows for observation, and the needle is connected to a constant vacuum (about 0.01 mm-Hg). A negative crystal grows at the end of the needle.

The preparation time for each crystal is about 15 minutes. Fewer than one out of ten blocks is rejected because of cracking or elastic strain (visible between crossed polaroids). The most difficult part of the procedure is to make a vacuum-tight connection to the needle without breaking the bond of needle to ice. In making the connection with the standard ground-glass syringe that we used, one must use only pressure—rotation is likely to free the needle from the ice.

Measurement of the extension of an isolated corner of a negative crystal (the junction of two prism faces with one basal face, none of which intersect the needle) in the *a*- and *c*-axis directions as a function of time can be made at various temperatures. The four habit changes of snow crystals also occur in the negative crystals at roughly the same temperatures (see Fig. 1).

The evaporation is a process which occurs in steps, as does crystal growth. In negative crystals skeletal growth of the prism faces (Figs. 1*a*, 2, 3) and of the basal face (Fig. 1*b*) is common when the linear growth at the corners exceeds about 2 mm/hour. The controlling factor is heat diffusion to the corners and edges, while in skeletal growth of positive crystals from vapor, the controlling factors are heat diffusion from the corners and edges and vapor diffusion to them.

Evaporation of ice in a vacuum produces crystal faces when the surface is concave, but usually not when it is convex (Fig. 2), because of both availability of steps and heat flow. For growth of positive ice crystals in a vacuum the reverse presumably would be true if one could maintain the difference in heat conductivity between the growing crystal and its environment. Unfortunately, the sign of this difference must also be reversed, and it is much more difficult to produce crystal faces when growing positive ice

crystals in a vacuum, since the surfaces tend to be isotherms around the heat sink.

The gas within a growing negative crystal is almost pure water vapor. Thus, because of the high vapor pressure of ice, we can assume that the surface of a growing negative crystal has an approximately uniform (though not usually constant) temperature. A nonuniform surface temperature is rapidly compensated by evaporation-condensation processes, for any temperature difference produces a corresponding difference in pressure. Nakaya (5) has shown that negative crystals migrate at appreciable speed with temperature gradients as small as $0.01^{\circ}\text{C}/\text{cm}$. Therefore, the main experimental difficulty in measuring relative evaporation rates is to maintain a uniform external temperature. Otherwise the negative crystals become asymmetrical, or even migrate (Fig. 3). This fact has so far prevented our obtaining relative evaporation rates that are quantitatively reproducible, but extreme precau-

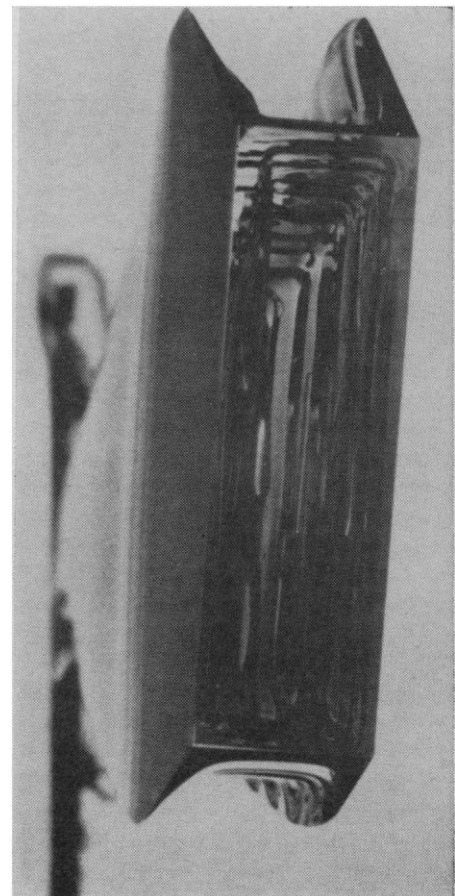


Fig. 3. This negative crystal is migrating toward the observer, away from the needle tip, as it grows in a temperature gradient. Needle diameter, 0.4 mm.

tions are not necessary when the purpose is only to produce good crystal faces for other experiments.

With negative crystal growth, surface contamination is automatically avoided, as is the need for elaborate pressure or temperature control. Ideally the surfaces would be the same as those produced by positive crystal growth.

CHARLES A. KNIGHT

NANCY C. KNIGHT

National Center for Atmospheric Research, Boulder, Colorado

References and Notes

1. Z. Yosida *Low Temp. Sci. Ser. A* **12**, 143 (1954); T. Nei, *Nature* **192**, 1177 (1961).
2. H. Kramers and S. Stemerding, *Appl. Sci. Res. Sect. A* **3**, 73 (1951); R. F. Strickland-Constable and E. W. Bruce, *Trans. Inst. Chem. Engrs. (London)* **32**, 192 (1954).
3. K. Higuchi, *Acta Met.* **6**, 636 (1958).
4. D. Kuroiwa and W. L. Hamilton, in *Ice and Snow*, W. D. Kingery, Ed. (M.I.T. Press, Cambridge, 1963), p. 34.
5. U. Nakaya, "Properties of single crystals of ice, revealed by internal melting," *Snow, Ice, Permafrost Res. Estab. Res. Pap. 13* (1956).
6. The crystals were collected during an expedition from the University of Hokkaido in 1964, led by Prof. A. Higashi, who furnished the crystals used in this work and measured their dislocation density.
7. Work done at the Ice Research Laboratory, Department of Applied Physics, Hokkaido University, Japan and supported partially by NSF and the Japan Society for the Promotion of Science, as part of the Japan-U.S. Cooperative Science Program. Primary support was from the National Center for Atmospheric Research. Criticism and help from A. Higashi, co-researcher on the cooperative program, members of his laboratory, and members of the Institute of Low Temperature Science are gratefully acknowledged.

25 August 1965

Autoradiography: Technique for Drastic Reduction of Exposure Time to Alpha Particles

Abstract. *High-speed, gross, alpha autoradiographs can be made if silver-activated zinc sulfide is used as an intensifier in conjunction with high-speed film. The intensifier is interposed between the sample and film. This technique requires about 1/1000 of the exposure time required with Kodak NTB plates. The gross autoradiographs have greater contrast but slightly less resolution than conventional plates.*

High-speed autoradiographic technique is sought when exposure time is the prime consideration or when the radiation level is too low for conventional methods to be practical. We describe the use of silver-activated ZnS as an intensifier to reduce exposure time for gross alpha autoradiography.

When a 5-Mev alpha particle strikes a nuclear film, probably no more than 0.1 percent of the energy is utilized by the emulsion to produce the useful latent image. Since no more than 90 ev are required to produce a developable silver halide grain (1), and since alpha tracks rarely have more than 50 silver grains, over 99 percent of the alpha energy is ineffective in formation of a latent image. Use of phosphorescent ZnS crystals may reduce the direct effects of alpha particles on the film, but the radiation of light, which is efficient in producing a latent image compensates for the reduction. Thus, when a ZnS-augmented autoradiograph is made by an alpha emitter, the film may not receive the alpha radiation, but will receive a large quantity of photons from the excited ZnS crystals; consequently exposure time to attain a given grain density is reduced.

Silver-activated, microcrystalline ZnS is superior in radiation amplification to other combinations such as copper-activated ZnS or a mixture of ZnS and CdS. The phosphor finally selected was ZnS:Ag P7-920B (2) which is an efficient intensifier; it has desirable characteristics, such as wettability and uniformity of grain size.

About 25 g of phosphor was added to 100 ml of 2 percent gelatin solution. The coarse particles were allowed to settle out from the warmed solution for 1 to 2 minutes. The suspension was then decanted and coated directly onto the mounted specimen or deposited by sedimentation on a double-sided, aluminum-coated Mylar film (3) or thin plastic (such as Saran wrap). A uniform deposition of 12 to 14 mg/cm² was found to be optimum. Although the aluminum-coated Mylar film absorbs more alpha energy than one without backing, the absorption loss was offset by the reflection of light from the aluminum coating. The dried film was sandwiched between the photoemulsion and the specimen (Fig. 1, top) and exposed for a suitable period. By arranging the ZnS:Ag and photographic film on aluminum-coated Mylar film into a single light-tight unit, exposure can be carried out in full light. The ZnS:Ag on an aluminum-coated Mylar film can be made light-tight by taping it to the Polaroid film holder with the ZnS:Ag side adjacent to the photographic film (Fig. 1, bottom). Such a unit can be repeatedly used as long as the ZnS and

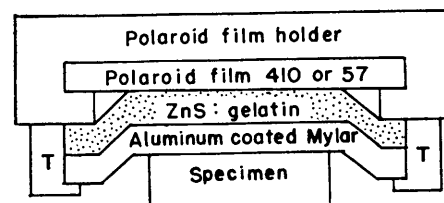
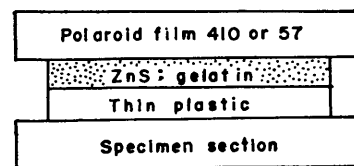


Fig. 1. (Top) Phosphor-film arrangement. (Bottom) Arrangement of a light-tight unit for daylight exposure. T, light-tight tape.

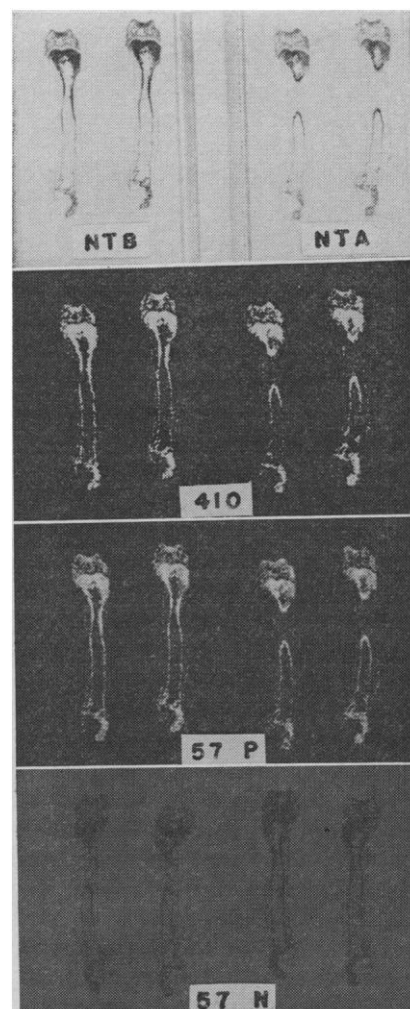


Fig. 2. Rat femur sections with ²³⁹Pu deposition were autoradiographed with NTB and NTA plates by conventional techniques. Then the same femur sections were used in the new technique. The exposure times were: 265 hours for NTB, 361 hours for NTA, 10 minutes for Polaroid Polarscope 410, 15 minutes for Polaroid Land 57 positive, and 15 minutes for Polaroid Land 57 negative (developer removed with Polaroid coating fluid).